

Establishment and characterization of fibroblast cell lines from the skin of the Yangtze finless porpoise

Jingzhen Wang · Weiting Su · Wenhui Nie ·
Jinhuan Wang · Wuhan Xiao · Ding Wang

Received: 24 April 2011 / Accepted: 18 August 2011 / Published online: 30 September 2011 / Editor: T. Okamoto
© The Society for In Vitro Biology 2011

Abstract The Yangtze finless porpoise (*Neophocaena phocaenoides asiaorientalis*), as the sole freshwater subspecies of *N. phocaenoides*, is endemic to the Yangtze River and its adjacent lakes. Its population has declined significantly over recent decades. In this study, we established a skin-derived finite fibroblast cell line of the Yangtze finless porpoise, named YFP-SF1, using primary cell culture methods, and an immortalized cell line, T-YFP-SF1, through co-transfection (GFP and SV40 T antigens) techniques. YFP-SF1 proliferated continuously with a minimum population doubling time of 31 h and exhibited age-dependent changes in growth rate. T-YFP-SF1 cells exhibited fibroblast morphology and were characterized by a shorter doubling time, higher attachment efficiencies, colony formation at a low seeding density, and growth in low serum concentrations. Anchorage independence and foci formation in the cell monolayer were observed from passage 36. The chromosome number of YFP-SF1 and T-YFP-SF1 remained stable at $2n=44$ in the early passages, and the viability of thawed cells remained above 90% after cryopreservation in liquid nitrogen. Taken together, we

have established fibroblast cell lines of Yangtze finless porpoise for the first time, which might assist as an in vitro model for this endangered mammal.

Keywords Finless porpoise · Fibroblast cell line · Co-transfection · In vitro

Introduction

The Yangtze River is the third longest river in the world. Two different freshwater cetacean species exist in the middle and lower reaches of the river and its adjacent lakes: the Yangtze River dolphin (*Lipotes vexillifer*, Baiji in Chinese) and the Yangtze finless porpoise (*Neophocaena phocaenoides asiaorientalis*) (Gao and Zhou 1995). They have been described as sentinels for the health of a river ecosystem (Stone 2010), allowing the early recognition of adverse impacts (Bossart 2006).

Both species have been dramatically affected by human activities and are facing an acute and severe situation (Wang 2009). Most recently, the Yangtze River dolphin (*L. vexillifer*), an obligate freshwater odontocete known only from the Yangtze River system, has been declared as “likely extinct” (Dalton 2006; Guo 2006; Turvey et al. 2007). The Yangtze finless porpoise, the sole freshwater subspecies of *N. phocaenoides*, has been listed as an endangered species (EN C2b) in the IUCN Red Data Book since 1996 (Baillie and Groombridge 1996) and has now been listed in the First Order of the National Key Protected Wild Aquatic Animals List in China. Its population has been decreasing annually at a rate of 5% or more (Zhao et al. 2008). An exhaustive survey conducted in 2006 by experts from seven countries found that the population of the Yangtze finless porpoise in the main river stem was approximately

J. Wang · W. Xiao (✉) · D. Wang (✉)
Key Laboratory of Biodiversity and Conservation
of Aquatic Organisms, Institute of Hydrobiology,
Chinese Academy of Sciences,
Wuhan 430072, People’s Republic of China
e-mail: w-xiao@ihb.ac.cn
e-mail: wangd@ihb.ac.cn

W. Su · W. Nie · J. Wang
State Key Laboratory of Genetic Resources and Evolution,
Kunming Institute of Zoology, Chinese Academy of Sciences,
Kunming, Yunnan 650223, People’s Republic of China

J. Wang
Graduate School of the Chinese Academy of Sciences,
Beijing 100039, People’s Republic of China

1,000~1,200 individuals, which was less than half of the population size estimated from the surveys from the year 1984 to 1991, and that the distribution is becoming more fragmented (Zhao et al. 2008; Wang 2009). Immediate, proactive, and effective measures must be taken to prevent the Yangtze finless porpoise from following the fate of the Baiji (Wang et al. 2006).

Extinction, being the irreversible loss of species, can profoundly jeopardize an ecosystem, which is one of the most alarming symptoms of the ongoing biodiversity crisis (He 2009). Maintaining and, if necessary, increasing biodiversity is the prime aim of conservation research (Leon-Quinto et al. 2009; Sutherland et al. 2009). Three conservation measures (in situ, ex situ conservation, and captive breeding) have been adopted to maintain and restore porpoise populations since the early 1990s by a Research Team of Conservation Biology of Aquatic Animals at the Institute of Hydrobiology, Chinese Academy of Sciences (Wang 2009). As a complementary supporting program to reinforce these three strategies, it is of significant scientific importance to establish a biological resources bank (Wiidt 1992; Holt and Pickard 1999; Comizzoli et al. 2000; Leon-Quinto et al. 2009), such as, the preservation of individual animals, semen, embryos, blood, tissue, cells, genomic libraries, and cDNA libraries. One of the most effective approaches is the establishment of somatic cell lines using cryopreservation (Shi 1989; Li et al. 2009). It provides a viable, practical, and timely backup of genetic material while it also overcomes the limitations of animal experiments. Moreover, the established cell lines will provide a promising tool for conservation research, including virological, toxicological, and epidemiological studies, as well as allowing future opportunities through different reproductive techniques, such as animal cloning.

Cetacean cells have historically been difficult to grow in culture (Andrews et al. 1973; Smith et al. 1987). Currently, only a few cetacean cell culture systems have been described, such as those derived from the beluga whale (*Delphinapterus leucas*) (Nielsen et al. 1989) and Atlantic bottlenose dolphin (*Tursiops truncatus*) (Carvan et al. 1994; Pine et al. 2004; Yu et al. 2005). In vitro somatic cell cultures have been applied in toxicological (Carvan et al. 1995; Pine et al. 2007; Wise et al. 2008), epidemiological (Kadoi et al. 1992; Buck et al. 1993), and cytogenetic studies (Walen and Madin 1965; Duffield et al. 1991; Heinzelmann et al. 2008). With the exception of successfully cultured lines, such as DKN1 (Pine et al. 2004) and DS1 (Yu et al. 2005), continuous cell strains have not yet been obtained, which may restrict the use in long-term studies. To our knowledge, no reports describing a successful cell line from freshwater cetaceans have been published.

In this study, a primary cell line YFP-SF1 (a skin fibroblast cell culture from a porpoise) and an immortalized cell line T-YFP-SF1 (a transfected cell strain derived from YFP-SF1) were established from the tail fluke skin of a Yangtze finless porpoise, using primary explants and the co-transfection of plasmids (pEGFP-N3 and pW2-Tt). The expression of transfected exogenous genes was detected and the growth property, karyotype, and cytological characteristics of the cell line were evaluated, as well as the detection of microorganisms.

Materials and Methods

Micro-invasive tissue collection. A tail fluke skin sample was obtained on 3rd April 2008 from a healthy male adult porpoise during a capture–release health assessment project in the ShiShou Tian-E-Zhou Nature Reserve (29°46'71"–29°51'45" N, 112°31'36"–112°36'90" E). For the skin biopsy, the sample site of the fluke margin was surgically scrubbed and sterilized. The strip sample (approximately 1.5×0.5 cm in size) was sheared off aseptically from the margin of the fluke close to the median notch and placed into a prepared tube containing Dulbecco's modified Eagle's medium (DMEM) with penicillin (2×100 U/ml), streptomycin (2×100 µg/ml), and amphotericin B (5 µg/ml). The incision on the fluke was surgically scrubbed with surgical cotton containing povidone iodine and a haemostatic and anti-inflammatory ointment. The porpoise was released and observed after homeostasis was achieved. The sample was transferred to the tissue culture laboratory within 12 h.

Primary cell culture. The skin specimen was rinsed and then finely chopped into approximately 1 mm³ pieces. During dissection, adipose, vascular, and necrotic tissues were removed. Approximately 30 fragments were distributed uniformly into 25 cm² tissue culture flasks. The flasks were inverted and then turned over after 2 h at room temperature to allow cellular attachment. The tissue pieces were fed with 5 ml of growth medium (DMEM and Ham's F12 in a 1:1 ratio supplemented with 20% fetal bovine serum (FBS), 100 U/ml penicillin, 100 µg/ml streptomycin, and 2 mM L-glutamine), adjusting the medium osmolality approximately at the level of 310~320 mOsm/l (in the range of the plasma osmolality of Yangtze finless porpoise) and the pH to approximately 7.4. The flasks were incubated at 37°C (rectal temperature of the porpoise) in a 5% CO₂, full humidity atmosphere and cell growth were monitored daily by an inverted microscope (Olympus CKX41). After the formation of a cell monolayer, the tissue fragments were dislodged from the flasks and attached to new flasks. The confluent cells were rinsed twice with phosphate-buffered

saline (PBS) to remove all traces of trypsin inhibitors. Trypsin solution (0.25%) was added to the side of the flasks until the cell monolayer was completely covered. The flasks were incubated, with the flasks lying flat, until the cells rounded up. The flasks were shaken gently to detach the cells, and 2 ml growth medium were added to each flask to block trypsinization. Cells were counted with a cytometer, diluted to the appropriate seeding concentration, and seeded into new flasks. Subsequent subcultures were performed according to above procedure every 7~9 d at a cell split ratio of 1:2~3. The primary cell line was named YFP-SF1.

Transfection of five fluorescent protein genes in YFP-SF1. Five fluorescent proteins (pEGFP-C1, pEGFP-N3, pEGFP-N1, pEYFP-C1, and pDsRed2-N1; Clontech) were transfected into YFP-SF1 cells mediated by Lipofectamine2000 following the protocol provided by the manufacturer. The transfection efficiencies were estimated with the use of a laser scanning microscope (Zeiss, LSM 510 META) after 24 h.

Cell immortalization. The plasmids, pEGFP-N3 and pEGFP-C1, and the pW2-Tt plasmid were co-transfected into the primary cell line YFP-SF1 using the method described above. The pEGFP-N3, pEGFP-C1 and pW2-Tt plasmids were mixed at a ratio of 8:1 and a total of 4~4.5 μ g DNA was used for the initial transfection. Cells expressing the transfected genes became visible as foci or clones. Several clones were picked and propagated in a selective medium. Each individual cell population was cultured continuously at a split ratio of 1:10. During this time, cryopreservation was carried out and the immortalized cell line (named T-YFP-SF1) was obtained.

The ability of YFP-SF1 and T-YFP-SF1 to withstand freezing in liquid nitrogen was determined in the cell growth state and freezing medium according to a previously described technique (Freshney 2005).

Karyotype analysis. The metaphase preparations were made from the second passage fibroblast of YFP-SF1. Colcemid was added to subconfluent cells at a concentration of 0.05 μ g/ml for 2 h, before the cells were harvested for chromosomal analysis. After incubation, the cells were detached from the flask through trypsinization and subjected to hypotonic treatment with 0.075 M KCl for 10~15 min. Subsequently, the cells were fixed three times using Carnoy's fixative (3:1 of methanol:glacial acetic acid) and slides were prepared by standard air drying technique. G-banding was performed according to the trypsin/Giemsa staining procedure (Seabright 1972) and was modified to facilitate specific identification of all homologs. Slides were kept at 60~65°C for 3 h and were trypsinized for 3~8 min in a 1:50 (2.5% trypsin/PBS) trypsin solution at room

temperature and rinsed twice with PBS. Finally, the slides were stained with Giemsa stain diluted 1:50 with Gurr's buffer (pH 6.8) for 2~5 min, washed with tap water, and air dried.

Detection of SV40 large T and small t. To determine whether larger T (LT) and small t (ST) proteins were expressed in T-YFP-SF1, a reverse transcription PCR was employed. Total RNA was extracted from T-YFP-SF1 cells (passage 10 and passage 40), COS-7 cells (SV40-transformed simian kidney cells, positive control) and YFP-SF1 cells (negative control) by using an RNAPrep pure cell/bacteria kit (Tiangen Biotech, Beijing, China), according to the manufacturer's protocol. RNA quality control was conducted using gel electrophoresis in a 1.5% agarose-denaturing gel and optical density measurements were made with a NanoDrop ND-1000 Spectrophotometer. First-strand cDNA was synthesized from total RNA using a First-Strand cDNA Synthesis Kit (Fermentas, Hanover United States). The cDNA served as a template for PCR amplification, using the primers in Table 1.

PCR cycling conditions were melting at 94°C for 5 min followed by 30 cycles of 94°C for 30 s, 48°C for 30 s, and 72°C for 1 min, followed by one cycle of 72°C for 5 min.

Western blot for the detection of SV40 LT antigen and ST antigen. Samples were prepared from controls (COS-7 cells as a positive control, non-transfected cells as negative control) and T-YFP-SF1 cells (passage 14 and passage 45). Proteins were separated by SDS polyacrylamide gel electrophoresis and transferred onto a polyvinylidene fluoride membrane using a semi-dry blotting technique. The primary monoclonal antibody SV40 T Ag Pab108 (Santa Cruz Biotechnology, Inc., Santa Cruz, CA) and the secondary antibody goat anti-mouse IgG-HRP polyclonal (Santa Cruz Biotechnology, Inc., Santa Cruz, CA) were applied for the detection of LT and ST.

Immunofluorescence assay. T-YFP-SF1 (passage 7 and passage 40) cells and control cells (cos-7 cells and YFP-SF1 cells) were grown on sterile glass cover slips in 6-well plates overnight until cells reached 60~80% confluence. After fixing the cells with 4% paraformaldehyde for 10 min at room temperature, the primary antibody SV40 T Ag Pab108 (Santa Cruz) and the fluorescence-labeled secondary

Table 1. SV40 LT and ST primers used in the present study

Name	Sequence (5' to 3')	Position
SV40 LT-F	CATGCTCCTTTAACCCACCT	4,052–4,071 bp
SV40 LT-R	CATCCTGATAAAGGAGGAGATG	5,019–5,041 bp
SV40 ST-F	CGAAGCAGTAGCAATCAACC	4,740–4,759 bp
SV40 ST-R	CATCCTGATAAAGGAGGAGATG	5,019–5,041 bp

antibody CY3-goat anti-mouse IgG (Invitrogen, Carlsbad, United States) were used to identify transfected T genes. The cover slips were rinsed with distilled water and sealed. As a negative control, the first antibody was omitted and the T-YFP-SF1 samples were incubated with secondary antibodies only to check for unspecific binding or for cross-reaction between the secondary antibodies.

Characterization of cell line properties. Growth properties of both YFP-SF1 and T-YFP-SF1 were characterized through a combination method, including growth curves, serum dependency detection, population doubling time, colony forming efficiency, anchorage-independent growth ability, and chromosome number analysis. The growth capacity and serum dependency of YFP-SF1 (passage 7 and passage 20) and T-YFP-SF1 (passage 20 after transfection) were evaluated using a 3-(4, 5-dimethylthiazol-2-yl)-2, 5-diphenyl-tetrazolium bromide (MTT; Sigma Aldrich, St. Louis, MO) assay (Mosmann 1983; Hansen et al. 1989; Wilson et al. 1990). Briefly, 1,000 cells (volume, 100 μ l/well) were seeded with serum concentrations of 15%, 10%, 5%, and 1% into 96-well plates and analyzed every 24 h, until 192 h after plating. At each time point, 20 μ l of filter-sterilized MTT (5 mg/ml in PBS) was added to each well and incubated for 5 h at 37°C. Media was removed and blue formazan crystals trapped in cells were dissolved in sterile DMSO (100 μ l) by incubating at 37°C for 30 min. Each analysis was carried out in triplicates. The absorbance was read on a multi-well scanning spectrophotometer (ELISA reader) at 570 nm as test wavelength and 690 nm as reference wavelength. Growth curves were plotted from the means of each treatment as optical density (OD, 570 nm) against the culture time (h). The population doubling times (PDT) of these three cell strains were calculated during the exponential growth phase of the cells according to the growth curve. Meanwhile, comparative analysis of the serum dependency and the attachment efficiency of these cells were also assessed. Differences in proliferation as response to the effect of serum concentration between the three cell cultures were assessed by two-way ANOVA followed by a post hoc test with Bonferroni correction, using the SPSS16.0 software package. A one-way ANOVA was used when one influencing factor had been selected ($p < 0.05$ was considered significant).

Low density cell colony formation, or plating efficiency, was tested according to the protocol (Freshney 2005). Single cell suspensions of YFP-SF1 (passage 10) and T-YFP-SF1 (passage 20) were prepared, and about 100 cells were plated in each well of 6-well plates (about ten cells/cm², three replicates at each cell line). The plates were incubated until colonies were visible under an inverted microscope (Olympus CKX41).

A soft agar colony assay was conducted according to the method of Pavelic et al. (1980) (Pavelic et al. 1980), to test whether T-YFP-SF1 cells had transformed activity. T-YFP-SF1 cells (passage 3, passage 20, and passage 42) and control cells (COS-7 and YFP-SF1) were resuspended in 0.34% low melting point agarose (LMP agarose, Promega, Madison, United States) in DMEM/F12 supplemented with 20% FBS and were plated in triplicates in a 6-well plate coated with 0.6% LMP agarose in DMEM/F12 plus 20% FBS at a cell number of 2.5×10^3 per well. Cultures were maintained in an incubator at 37°C, incubated for 30 d and cells were fed once a week. The cells were observed under an inverted microscope (Olympus CKX41).

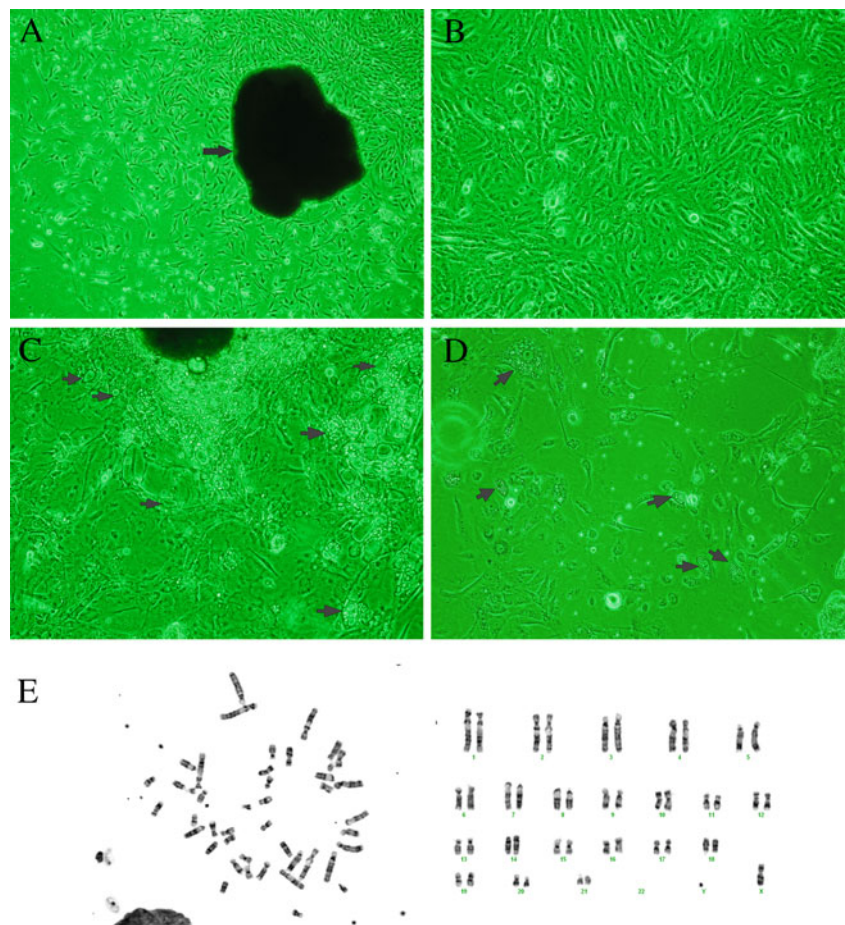
Metaphasic cells of YFP-SF1 at passage 17 and T-YFP-SF1 at passage 3, passage 20, and passage 36 were also prepared for the count of chromosome numbers and to estimate the genetic stability of cells.

Microorganism detection. Potentially harmful bacteria, yeasts, and other fungi were detected by the method described by Davis (Davis 2002). Antibiotic-free media testing and microbiological culture using tryptose soy broth and fluid thioglycollate medium were performed to test for the presence of aerobic, anaerobic, facultative anaerobic bacteria and fungi. A modified DIPA (4',6-diamidino-2'-phenylindole) staining method according to (Russell et al. 1975) was conducted to test for *Mycoplasma* spp. Briefly, prior to detection, T-YFP-SF1 and YFP-SF1 cells were cultured in antibiotic-free media for at least 1 wk or a minimum of two passages. When 60~70% confluence was reached, cells were harvested and suspended in PBS. One drop of suspension was placed on a microscope slide and air dried. This was washed once with DAPI-methanol (working solution, 1 μ g/ml), covered with DAPI-methanol and incubated for 20 min at 37°C. After washing with PBS, the cells were examined under a fluorescence microscope with DAPI filter (Zeiss, Axioplan 2 Imaging).

Results

A primary cell line of the Yangtze finless porpoise was obtained. A primary cell culture was established from the sample using primary explant technique. Cell migration from the edges of the explants was observed approximately 2 wk after the attachment of tissue fragments (Fig. 1A), and a cell monolayer formed on day 20. Afterwards, the first subculture was conducted at a 1:3 split ratio, all early passages of the cell cultures shared very similar growth patterns, and reached 90% confluence within 7 d (Fig. 1B). The primary culture system contained cells of mixed origins, including epithelial, spindle-shaped, and fibroblast

Figure 1. Cell morphology of YFP-SF1. *A*, Primary explant culture from Yangtze finless porpoise fluke skin biopsy, $\times 4$ objective; the black arrow marks a tissue fragment. *B*, Passage two cells, $\times 10$ objective. *C*, Intracellular lipid droplets in primary cell culture, which is special for cetacean cells, $\times 4$ objective. *D*, Intracellular lipid droplets could also be found in subculture cells, $\times 10$ objective. *E*, G-banded karyotypes of the Yangtze finless porpoise.



cells. The dark color of some cells was due to the considerable amount of melanin pigment in the porpoise skin (Fig. 1*B*) (Yu et al. 2005). In the progress of cell passages, the melanin density dropped off and the cytoplasm become gradually clearer. In certain stages of the early YFP-SF1 cell cultures, massive intracellular lipid droplets were found clustered in the perinuclear region or peripherally throughout the cytoplasm in many epithelial-like cells (Fig. 1*C, D* (indicated by arrows)). These unusual intracellular lipid droplets have not been observed in the epidermis of terrestrial mammals and may be specific to cells of cetaceans due to their aquatic lifestyle (Menon et al. 1986; Pfeiffer and Jones 1993; Reeb et al. 2007).

Cryopreservation was conducted using cells from early passages, with two flasks of cells being selected for a continued subculture. Cell viability of thawed cells was more than 90% after they were cryopreserved in liquid nitrogen. Following serial subcultivations, the cells appeared uniformly spindle shaped. After approximately 23 passages, cells exhibited a slower proliferation that may be associated with cellular senescence.

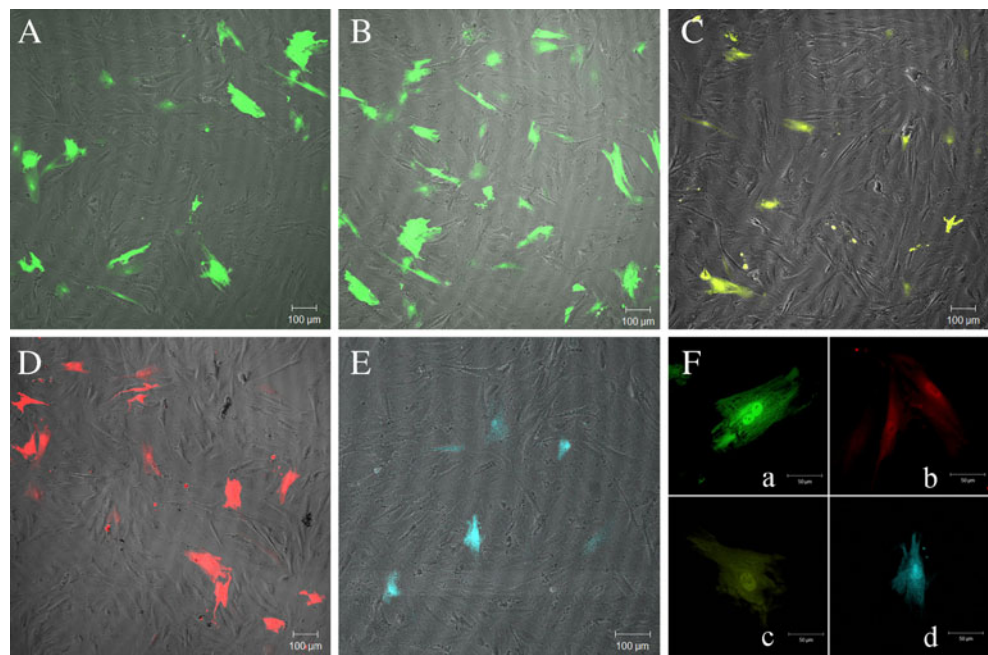
To determine whether the primary cell line was healthy, a karyotype analysis was performed. As shown in Fig. 1*E*, the porpoise chromosome number was $2n=44$, which

includes six pairs of metacentric chromosomes (m), seven pairs of submetacentric (sm), four pairs of subtelocentric (st), and four pairs of telocentric chromosomes (t). The X chromosome is metacentric and the Y chromosome is telocentric. Thus the chromosome pattern can be described as $2n=44$, male, XY, 13m+14sm+8st+9t.

To characterize the properties of the primary cell line further and to select an optimal fluorescent gene for subsequent co-transfection, the exogenous gene expression in this cell line was investigated under fluorescence microscopy (Fig. 2*A–F*). Meanwhile, the transfection efficiency was calculated (Table 2).

An immortalized cell line of the Yangtze finless porpoise was obtained. To obtain an immortalized cell line of Yangtze finless porpoise, the primary cell line YFP-SF1 was transfected with pEGFP-N3, pEGFP-C1, and pW2-Tt. G418 was used for selection and green fluorescent protein (GFP) was used as a marker for positive clones. Positive G418-resistant colonies of rapidly proliferating morphologically altered cells appeared within 24~30 d (Fig. 3*A1, B*). Using a limiting dilution method, the transfected cells were screened and proliferated. The cells could easily form fluorescence colonies (Fig. 3*C, E*) when seeded at low cell

Figure 2. The expression and distribution of five fluorescent proteins in YFP-SF1 cells at 24 h post-transfection. *A*, pEGFP-C1, *B*, pEGFP-N3, *C*, pEYFP-C1, *D*, pDsRed2-N1, *E*, pECFP-N1; *A–E*: Plan-Neofluar ×10/0.3 ph1 objective. *F*, Subcellular location of the fluorescent proteins in YFP-SF1: *a*, pEGFP-N3, *b*, pDsRed2-N1, *c*, pEYFP-C1, *d*, pECFP-N1; *a–d*: Plan-Neofluar ×20/0.5 objective.



density. Cultures from all transfected colonies proliferated at a faster rate than non-transfected cultures, and formed cell monolayers in 2 d after passaging at a 1:3 ratio (Fig. 3A2, D). One cell strain (T-YFP-SF1) was selected and proliferated for further studies. When T-YFP-SF1 was passing about 36 generations in vitro, formation of foci could be detected under an inverted microscope, which was not observed in earlier passages (Fig. 3A3).

Two Simian virus 40 early region (SV40 ER) proteins, LT and ST, are critical for cell immortalization and transformation (Fanning and Knippers 1992; Rundell and Parakati 2001). To test whether SV40 large T and small t were functional in the immortalized cell line, RT-PCR and a Western blot were employed for further assays. In the RT-PCR detection experiments, the quality assessment of total RNA using gel electrophoresis method (two bright bands, 28s and 18s) and NanoDrop ND-1000 Spectrophotometer (Table 3) showed the integrity and purity of the RNA. As shown in the schematic diagram of SV40ER in Fig. 4A, LT and ST shared the same N-terminal 82 amino acids (indicated by the red section, CDS “4,918–5,163 bp”), but each carried unique domains (LT—CDS “2,691–5,163 bp” containing the intron E_18S “4,572–4,917 bp”; ST—CDS “4,639–5,163 bp”). According to the CDS sequence of LT and ST, two pairs of primers were

designed (Table 1; Fig. 4A). Following RT-PCR amplification, electrophoresis was conducted. As shown in Fig. 4B, the expression of SV40LT and ST was detected (LT, 642 bp and ST, 302 bp) in T-YFP-SF1 cells. The band from PCR of pW2-Tt DNAs that amplified with the LT primers was approximately 1,000 bp long, including the 346 bp intron E_18s. Two bands (642 and 990 bp) were found in the RT-PCR of COS-7 and T-YFP-SF1 due to alternative splicing. In the detection of ST, both PCRs with pW2-Tt and RT-PCR with COS-7 cells and T-YFP-SF cells resulted in a 302 bp band, while the results of YFP-SF1 cells were negative. These results demonstrated the expressions of SV40 LT and ST in T-YFP-SF1 cells on the RNA level.

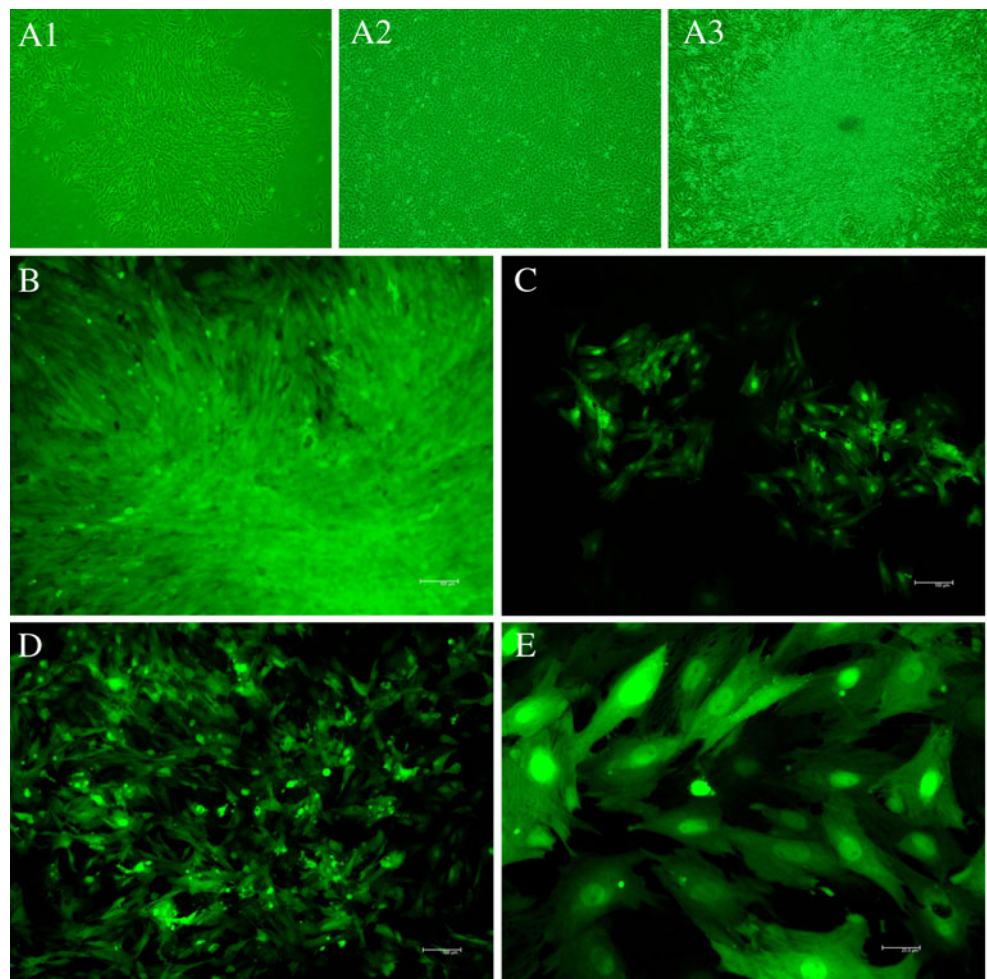
In a Western blot, as depicted in Fig. 4D, non-transfected YFP-SF1 cells showed no immunological; cross-reactivity with the antibody and no band was shown on the film, whereas COS-7 cells and T-YFP-SF1 cells cross-reacted with the anti-T(t) antibodies and two bands (94 kDa and 21 kDa) were exposed on the film.

To detect the co-occurrence relation of pW2-Tt and pEGFP-N3 (or C1) in T-YFP-SF1 cells, indirect immunofluorescence with SV40 T Ag Pab108 (specific for SV40 LT and ST) was carried out. A fluorescence-labeled secondary antibody CY3-goat anti-mouse IgG (red fluorescence) was

Table 2. Transfection efficiencies of five fluorescence genes and the co-transfection efficiencies

Transfection time (h)	Five fluorescent protein genes transfection rate (%)					Co-transfection rate (%)
	pEGFP-C1	pEGFP-N3	pDsRed2-N1	pEYFP-C1	pECFP-N1	pEGFP-N3
24	24.3	28.9	23.7	20.6	8.4	15.7

Figure 3. Images of T-YFP-SF1. *A*, Observation under inverted microscope, $\times 4$ objective; *A1*, colony formed after co-transfection and screening, $\times 4$ objective; *A2*, subculture monolayer of T-YFP-SF1, the cells appeared smaller, more rounded and higher nucleus/cytoplasm ratio compared with nontransfected cells; *A3*, foci formation was detected in cell culture of T-YFP-SF-P36 (passage 36), $\times 10$ objective. *B*, Colony observation with fluorescence microscope. Scale bar, 100 μm . *C*, Colonies formation after passage at 1:10 ratio. Scale bar, 100 μm . *D*, Subculture cells of T-YFP-SF1. Scale bar, 100 μm . *E*, Clones formed in low density seeded. Scale bar, 25 μm .



introduced to display the expression of LT and ST through a stepwise reaction. As shown in Fig. 5, both green and red fluorescence could be observed in T-YFP-SF1 cells. In some cells, red and green fluorescence co-existed, but in some cells, only red fluorescence could be observed. The green fluorescence intensity in cells of passage 7 (Fig. 5A1, B1) was higher than in cells of passage 40 (Fig. 5A2, B2). Similar to the positive control COS-7 cells (Fig. 5C2, D1), T-YFP-SF1 (Fig. 5B1, B2, C1) cells showed distinct red fluorescent nuclei, whereas non-transfected YFP-SF1 cells (Fig. 5D2) and cells where the first antibody was omitted did not show a clear outline of the nuclei.

Transfection of SV40 LT and ST facilitated cell growth. The cell proliferation rates of YFP-SF1 cells (Fig. 6A, B) and

T-YFP-SF1 cells (Fig. 6C) in different serum concentrations were assessed using an MTT assay. Since the absorbance of the formazan produced by MTT is directly proportional to the number of live cells tested (Mosmann 1983; Wilson et al. 1990; Strickland et al. 1996), optical density (OD) was used to measure relative cell numbers. As shown in Fig. 6A–C, the growth curves of YFP-SF1 (A, B) and T-YFP-SF1 (C) cells appeared as a typical “S” shape with a latency phase of 48 h after cells were seeded. The cells then entered an exponential growth phase and reached a plateau phase at 120 h, with the exception of continuously growing T-YFP-SF1 cells. These three cell cultures exhibited different plateau densities (Fig. 6D; one-way ANOVA, $F=67.82$, $p<0.05$), cell attachment efficiencies (Fig. 6F; two-way ANOVA, $F=21.468$, $p<0.05$, $R^2=0.908$),

Table 3. Optical density measurements for RNA purity detection using a NanoDrop ND-1000 Spectrophotometer

Absorbance ratio	COS-7	YFP-SF1	T-YFP-SF1-P10	T-YFP-SF1-P40
A260/280	2.08	2.10	2.03	2.07
A260/230	2.08	2.01	2.12	2.15

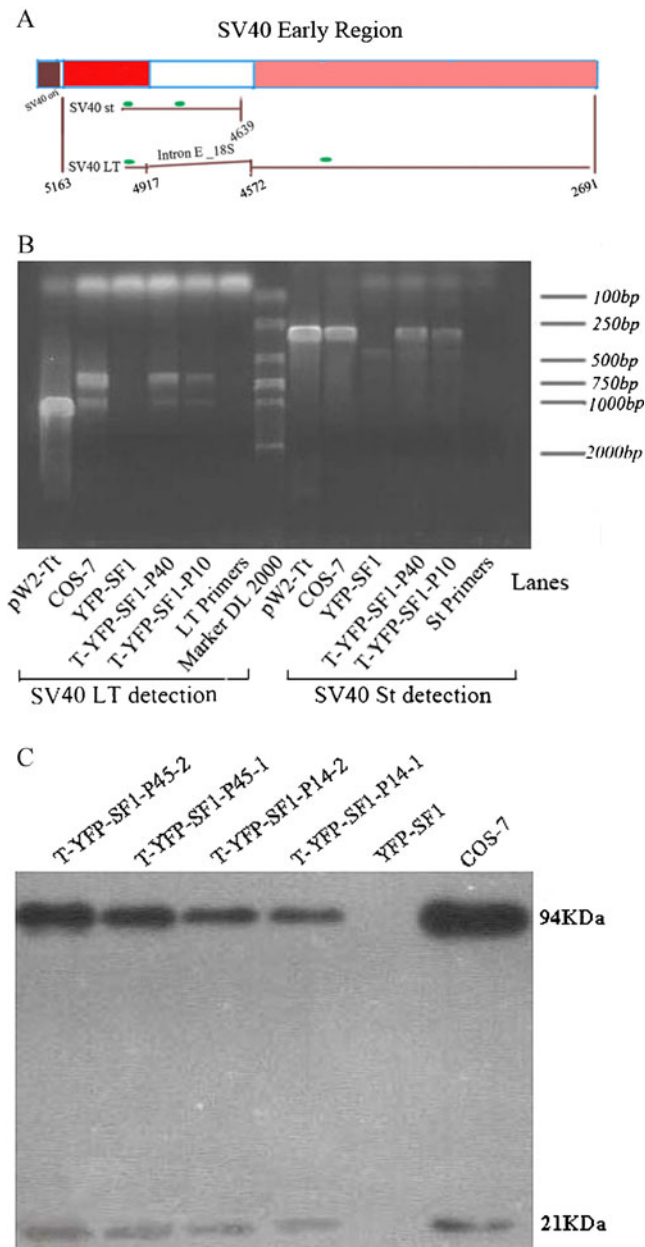


Figure 4. Detection of the expression of transfected SV40 large T antigen and small t antigens, using reverse transcription PCR and western blot. *A*, Schematic diagram of the SV40ER and the alternatively spliced proteins LT and ST. The number refers to the SV40 genomic coding sequence number. *B*, The detection of transfected SV40LT and ST using reverse transcription PCR. PCR with pW2-Tt DNA to amplify SV40 ER including LT exons and intron and ST, as positive control; RT-PCR with COS-7 cells RNA to amplify SV40 LT and ST transcript, as positive control; RT-PCR with YFP-SF1 cells RNA, as negative control; RT-PCR with T-YFP-SF1-P40 (passage 40 after transfection) and T-YFP-SF1-P10 (passage 10 after transfection) cells RNA to amplify SV40 LT and ST transcript; LT primers and ST primers, as negative control. The samples loading sites is on the bottom of this photo. *C*, Western blot of T-YFP-SF1, COS-7 was used as positive control, and YFP-SF1 was used as negative control.

and serum-dependent properties (Fig. 6E; two-way ANOVA, $F=227.05$, $p<0.05$, $R^2=0.986$). T-YFP-SF1

showed a significantly higher plateau density and attachment efficiency than YFP-SF1 (passage 7 and passage 20) at the same serum level. YFP-SF1 cells (especially cells from passage 20) grew slowly in 5% serum and could not grow in 1% serum, while T-YFP-SF1 cells could proliferate consistently with low serum concentrations. The PDT of YFP-SF1 and T-YFP-SF1 at normal serum levels (15% and 10%) were calculated using the algorithm provided by <http://www.doubling-time.com/compute.php> (Widera et al. 2009). The results are shown in Fig. 6G. When using the relative cell number and the OD value, and the amount of cells was replaced, the resulting PDT was identical. The total number of cells (N_t) at a given time (t) following inoculation is given by $N_t=N_i*2^n=N_i*e^{rt}$, where N_i is the number of cells inoculated, n is the generation number that cells had experienced through the time t , and r is the multiplication rate. From the formula, it can be deduced that $r = \ln \frac{N_t}{N_i} / t$. PDT is the time, expressed in hours, taken for cell number to double, so

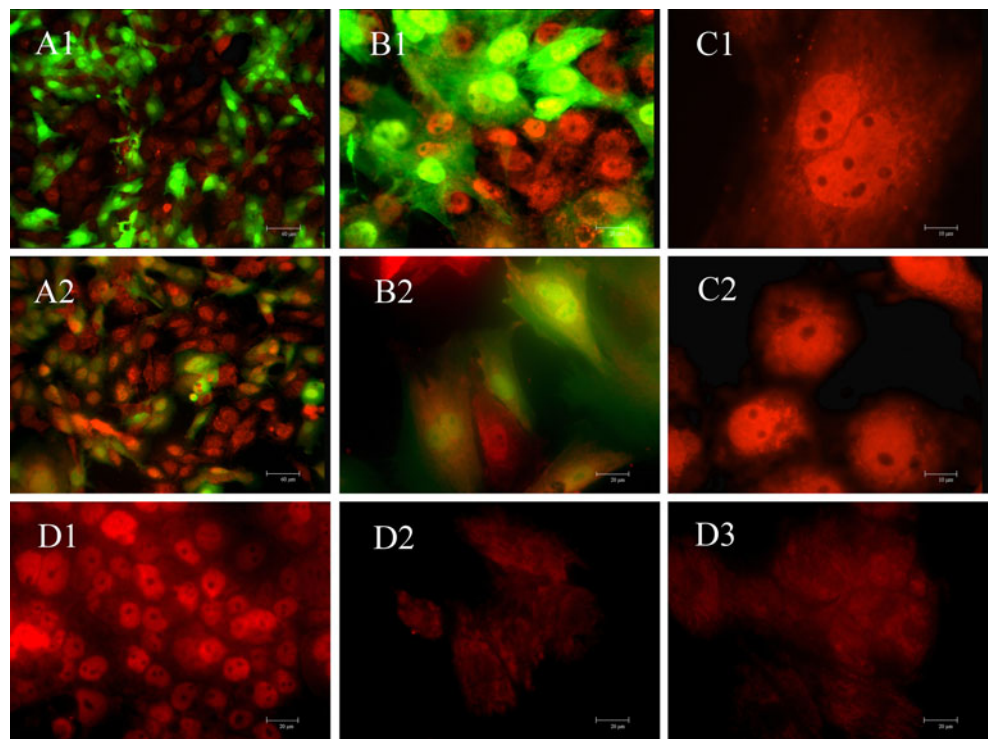
$$\frac{PDT}{\ln(2)} = \frac{t}{\ln\left(\frac{N_t}{N_i}\right)} \text{ and } PDT = \frac{t * \ln(2)}{\ln\left(\frac{N_t}{N_i}\right)} = \ln(2) / r.$$

As the absorbance of formazan is directly proportional to the cell number, N_t/N_i can be replaced by OD_t/OD_i . As shown in Fig. 6G, the exponential growth equations of YFP-SF1-P7, YFP-SF1-P20 and T-YFP-SF1-P20 with 15% serum were as follows: relative cell amount= $0.030*e^{0.22*t}$, $0.033*e^{0.014*t}$, $0.048*e^{0.025*t}$, and the PDT was 31.45 h, 50.24 h, and 27.78 h, respectively, which were shorter than in 10% serum (Table 4). The results indicated that YFP-SF1 growth decreased, with continuous passing in vitro while the transfection of SV40LT and ST facilitated the growth of the porpoise cells.

To analyze the cell proliferation and survival ability of YFP-SF1 and T-YFP-SF1 further, approximately 100 cells per well were seeded in 6-well plate. Two weeks later, T-YFP-SF1 colonies could be observed with a plating efficiency of 0.53 ± 0.06 (mean \pm STD) while colonies could not be observed in the three replications of YFP-SF1 passage ten cells.

The anchorage-independent growth property of T-YFP-SF1 was examined in soft agar. Within COS-7 cells, colonies were larger in size and were visible under a microscope after 2 wk (Fig. 7A), 5 d earlier than colonies formed by T-YFP-SF1-P42 (Fig. 7C). YFP-SF1 (Fig. 7B), T-YFP-SF1-P20 (Fig. 7E), and T-YFP-SF1-P3 (Fig. 7F) did not form colonies after 4 wk. At this time point, parts of T-YFP-SF1-P42 cell pellets proliferated and coalesced into mulberry-shapes or spherical cell masses of varying sizes (Fig. 7D).

Figure 5. Detection of the co-existence of SV40 T(t) antigen and GFP, using immunofluorescence assay. *A1, B1*: T-YFP-SF1 cells, passage 7. Scale bars, 60 and 20 μm , respectively. *A2, B2*: T-YFP-SF1 cells, passage 40. Scale bars, 60 and 20 μm , respectively. *C1* Location of T antigen in T-YFP-SF1 cells, the nuclei are bright red fluorescent. Scale bar, 10 μm . *C2*, Location of T antigen in COS-7 cells. Scale bar, 10 μm . *D1*, Detection of expression in COS-7 cells as positive control; *D2*, YFP-SF1 cells, negative control, *D3*, T-YFP-SF1 cells omitted the first antibody, negative control. Scale bar, 20 μm .



The majority of the YFP-SF1 (passage 7) and T-YFP-SF1 (passage 3, 20, and 36) cells that were tested for chromosome numbers were diploid ($2n=44$), and remained stable (data not shown). The transfection did not cause any obvious chromosome number changes at the early passage of T-YFP-SF1, with 87% being diploid at passage 20. However, the proportion of aneuploid cells increased by passage 36, at which time the cells exhibited the transformed characteristics of foci formation on the background of a monolayer, colony formation in soft agar.

YFP-SF1 and T-YFP-SF1 were negative for microbial infections. The YFP-SF1 and T-YFP-SF1 cell lines were cultured in antibiotic-free medium and in two types of microbiological medium for at least 1 wk. No turbidity or other visible changes were observed, indicating that the newly established cell lines were not contaminated by bacteria or fungi. After staining with DIPA, the nuclei of the cells appeared as blue ellipses when observed under a fluorescence microscope (Fig. 7E1), whereas in *Mycoplasma*-infected cultures small dots or flecks of fluorescence could be seen around the cell nuclei, leading to a “starry sky” appearance (Fig. 7E2).

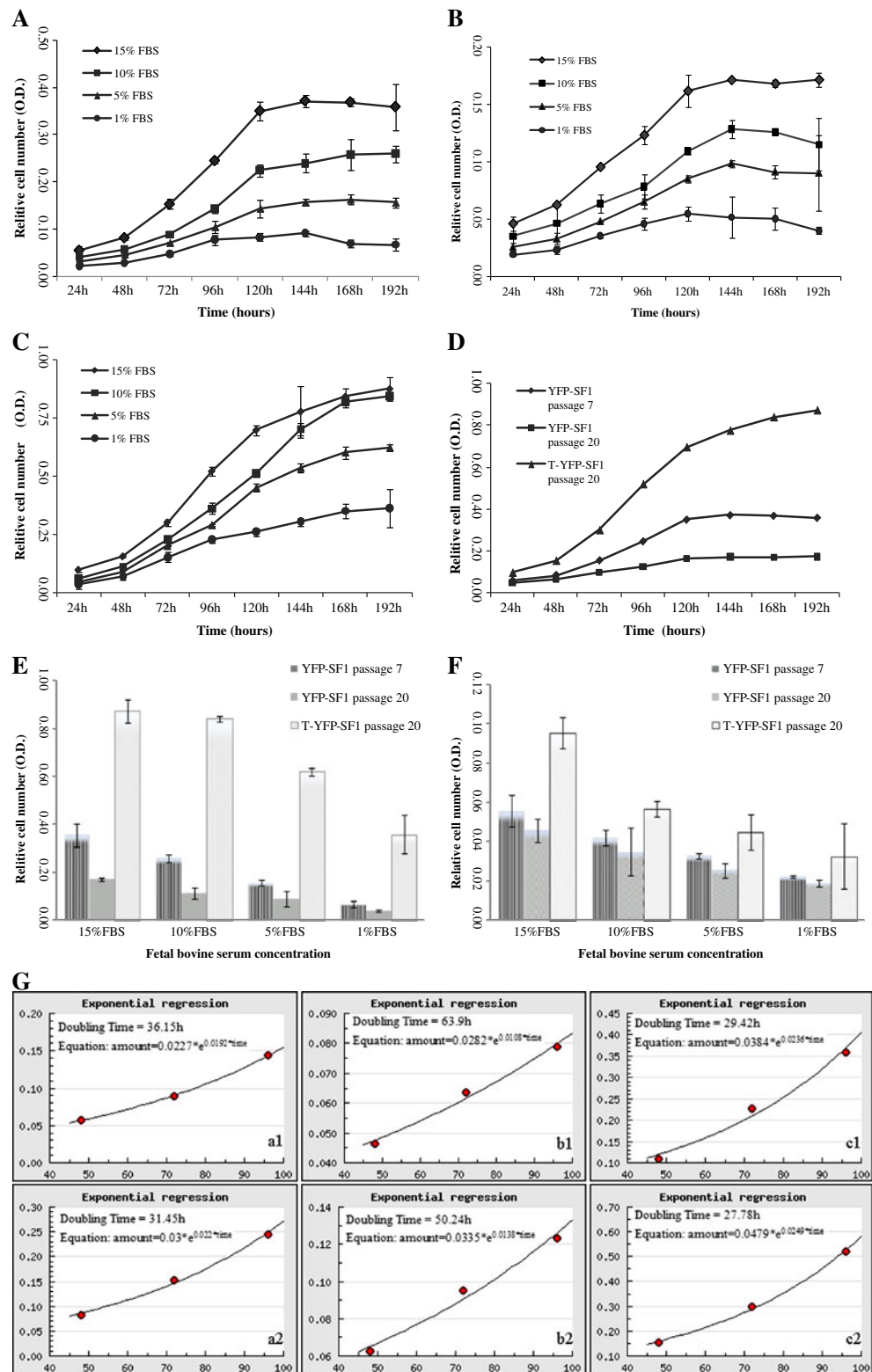
Discussion

The major challenges for establishing cetacean cell lines are to obtain fresh sterile samples and to overcome the barriers

for growing cells in vitro. To obtain fresh samples from these animals can prove very difficult due to their aquatic habitat and because of legal, logistical, and ethical restrictions due to their endangered status. Therefore, it is crucial to establish an effective micro-invasive sterile sampling technique. It has indicated that skin biopsies taken from the flank, dorsal area or near the dorsal fin of other cetaceans caused no obvious disturbance to the subjects' behavior (Brown et al. 1991; Fossi et al. 2000; Marsili et al. 2000; Wise et al. 2008), and did not result in physiological damage (Weller et al. 1997; Jefferson and Hung 2008). However, it was found that lesions on the skin of Yangtze finless porpoise did not heal easily. Thus, it was suggested that micro-skin biopsies from the fluke edge might be a feasible way to obtain tissue samples for cell cultures from cetaceans.

Cell lines such as BWK and CDK have been successfully established for other cetacean species. The media used for these cell lines contain high amounts of vitamins, amino acids and additional NaCl (Nielsen et al. 1989; Carvan et al. 1994), while the newly established cell cultures of the Yangtze finless porpoise do not require additional supplements with the exception of 2 mM L-glutamine. Most normal somatic primary cell cultures undergo limited mitotic divisions, which are defined as replicative senescence or irreversible growth arrest (Hayflick and Moorhead 1961; Stewart and Weinberg 2002; Stewart and Weinberg 2006). The finite and short lifespan limits the long-term availability of these cells for further research, and the re-establishment of primary cell cultures from explanted

Fig. 6 Cell proliferation assessments of YFP-SF1 cells and T-YFP-SF1 using MTT assay. *A*, Growth curves of passage 7 YFP-SF1 cells in DMEM/F12 supplemented with different concentrations of FBS; *B*, Growth curves of passage 20 YFP-SF1 cells in DMEM/F12 supplemented with different concentrations of FBS; *C*, Growth curves of passage 20 T-YFP-SF1 cells in DMEM/F12 supplemented with different concentrations of FBS; *D*, growth curves of YFP-SF1 cells (passage 7 and passage 20) and T-YFP-SF1 cells supplement with 15% fetal bovine serum; *E*, Relative cell numbers of YFP-SF1 and T-YFP-SF1 supplemented with different serum concentration at 192 h, which indicated the difference of their serum-dependent properties. *F* relative cell number at 24 h, indicating the attachment efficiency of YFP-SF1 and T-YFP-SF1; (*G*) Calculation of cell population doubling time using exponential regression method. *a1* and *a2*, YFP-SF1, passage 7, with 10% and 15% serum concentration, respectively; *b1* and *b2*, YFP-SF1, passage 20, with 10% and 15% serum concentration, respectively; *c1* and *c2*, T-YFP-SF1, passage 20, with 10% and 15% serum concentration, respectively.



tissue are usually expensive and time-consuming. One approach to escape the Hayflick limit and to extend the cell culture lifespan is the gene transfer of SV40 early

regions (Bikel et al. 1987; Silva et al. 1995; Hahn et al. 2002; Chen and Hahn 2003). After the co-transfection of plasmids GFP and pW2-Tt, T-YFP-SF1 exhibited the

Table 4. Population doubling time of YFP-SF1-P7, YFP-SF1-P20, and T-YFP-SF1-P20 cells supplemented with different concentration serum

Serum concentration	Population doubling time (h)		
	YFP-SF1-P7	YFP-SF1-P20	T-YFP-SF1-P20
15% FBS	31.45	50.24	27.27
10% FBS	36.15	63.9	29.42

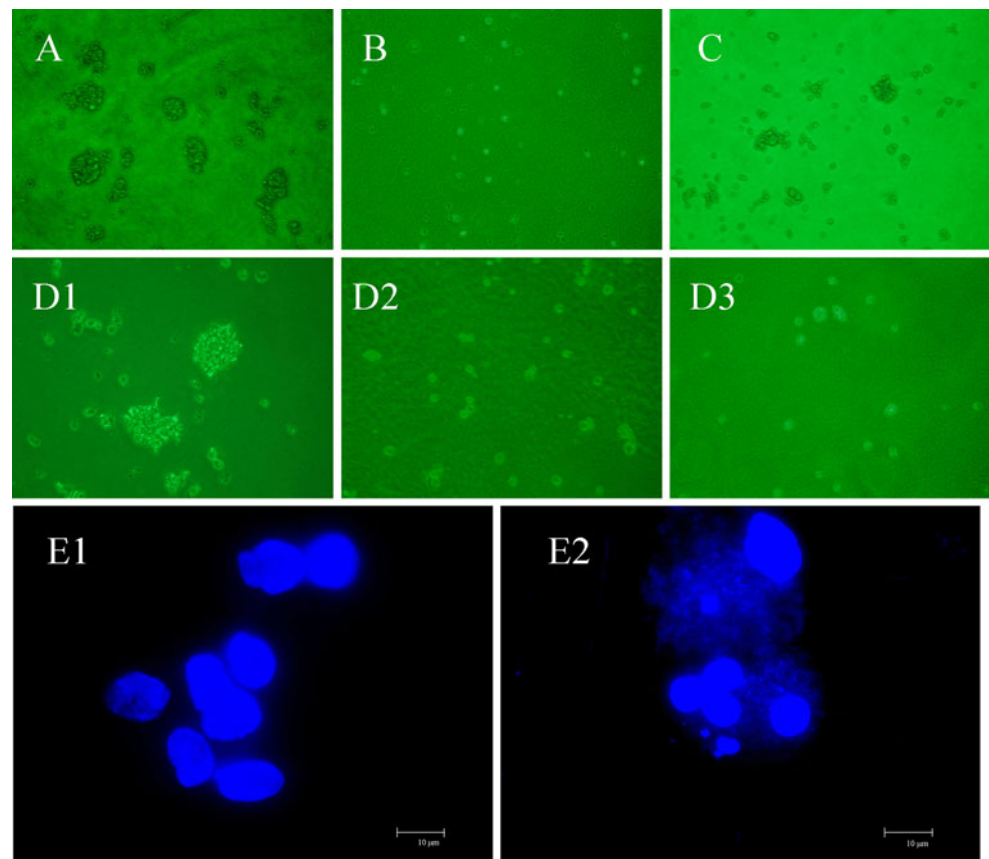
properties of immortalization, such as shorter doubling time, higher attachment efficiencies, colony formation in soft agar culture medium. In addition, the chromosome number of YFP-SF1 and T-YFP-SF1 remained stable at $2n=44$ in the early passages, and the viability of thawed cells remained above 90% after cryopreservation in liquid nitrogen. The successfulness in exogenous gene transfer and stable expression will encourage establishing iPS cells (inducible pluripotent cell) by transferring several important factors in cell reprogramming, which is important for species conservation.

The Yangtze finless porpoise, as the top predator and long-lived, long-term costal residents of the Yangtze River is the sentinel for the health of the aquatic ecosystem. Establishment of cell lines from the porpoise will provide the optimal in vitro model for the environment testing. In in vitro toxicology, the primary cell culture can keep the

characteristics as in vivo, but has a short lifespan and could lose the in vivo properties while the immortalized cell lines are longevity and retain the tissue-type specific features, which make the long-term studies possible (Bhagal et al. 2005). T-YFP-SF1 cells not only have the property of immortalization but contain the green fluorescent protein gene, which can monitor cell morphology under fluorescence microscope and facilitate toxicity testing.

In this study, we have tried a non-invaded method for establishing cell lines from the Yangtze finless porpoise, which might also be applied for some critical endangered species, such as vaquita (*Phocoena sinus*), (Jaramillo-Legorreta et al. 2007; Dalton 2010). The establishment of cell lines from endangered freshwater mammals facilitates population recovery. Combined with iPS cell techniques and animal cloning, we have the potential to recover the Yangtze finless porpoise population.

Figure 7. Soft agar colonies formation, karyotyping, and mycoplasma detection. *A*, Colonies formation of COS-7 cells in soft agar, photographed after 2 wk, $\times 10$ magnification, positive control; *B*, YFP-SF1 cells cannot form clones in soft agar, $\times 10$ magnification; *C*, clones of T-YFP-SF1-P42 cells, photographed after 3 wk, $10\times$ magnification. Clones detection of T-YFP-SF1-P42 (*D1*), T-YFP-SF1-P20 (*D2*), and T-YFP-SF1-P3 (*D3*) after 4 wk, $\times 20$ magnification. *E*, Cell preparations of T-YFP-SF1 and *Mycoplasma*-positive control stained with DAPI and viewed at $\times 630$ magnification using a fluorescence microscope; scale bar, 10 μm . *E1* *Mycoplasma*-negative T-YFP-SF1, only fluorescent nuclei can be seen in *E2* *Mycoplasma*-positive cells, presenting typical “starry sky” appearance.



Acknowledgments We are grateful to the individuals who participated in the finless porpoise capture–release project. This research was supported in part by the National Key Basic Research Foundation (973 Project; no. 2007CB411600), the National Natural Science Foundation of China (no. 30730018), and the Open Project of State Key Laboratory of Genetic Resources and Evolution (GREKF08-06).

References

- Andrews J.; Dill F. et al. The chromosome complement of the narwhal (*Monodon monoceros*). *Genome* 15: 349–353; 1973.
- Baillie J.; Groombridge B. IUCN red list of threatened animals. IUCN, Gland; 1996.
- Bhogal N.; Grindon C. et al. Toxicity testing: creating a revolution based on new technologies. *Trends Biotechnol.* 23: 299–307; 2005.
- Bikel I.; Montano X. et al. SV40 small t antigen enhances the transformation activity of limiting concentrations of SV40 large T antigen. *Cell* 48: 321–330; 1987.
- Bossart G. Marine mammals as sentinel species for oceans and human health. *Oceanography* 19: 134–137; 2006.
- Brown M.; Kraus S. et al. Reaction of North Atlantic right whales (*Eubalaena glacialis*) to skin biopsy sampling for genetic and pollutant analysis. *Rep. Int. Whal. Comm. Spec. Issue* 13: 81–89; 1991.
- Buck C.; Paulino G. et al. Isolation of St. Louis encephalitis virus from a killer whale. *Clin. Diagn. Virol.* 1: 109–112; 1993.
- Carvan M.; Flood L. et al. Effects of benzo(a)pyrene and tetrachlorodibenzo(p)dioxin on fetal dolphin kidney cells: inhibition of proliferation and initiation of DNA damage. *Chemosphere* 30: 187–198; 1995.
- Carvan M.; Santostefano M. et al. Characterization of a bottle-nosed-dolphin (*tursiops-truncatus*) kidney epithelial-cell line. *Mar. Mammal Sci.* 10: 52–69; 1994.
- Chen W.; Hahn W. SV40 early region oncoproteins and human cell transformation. *Histol. Histopathol.* 18: 541–550; 2003.
- Comizzoli P.; Mermillod P. et al. Reproductive biotechnologies for endangered mammalian species. *Reprod. Nutr. Dev.* 40: 493–504; 2000.
- Dalton R. Last hope for river dolphins. *Nature* 440: 1096–1097; 2006.
- Dalton R. Endangered-porpoise numbers fall to just 250. *Nature* 465: 674–675; 2010.
- Davis J. Basic cell culture. Oxford University Press Inc, New York; 2002.
- Duffield D.; Chamberin-Lea J. et al. Use of corneal cell culture for R-band chromosome studies on stranded cetaceans. *NOAA Tech. Rep. NMFS* 98: 91–100; 1991.
- Fanning E.; Knippers R. Structure and function of simian virus 40 large tumor antigen. *Annu. Rev. Biochem.* 61: 55–85; 1992.
- Fossi M.; Marsili L. et al. Skin biopsy of Mediterranean cetaceans for the investigation of interspecies susceptibility to xenobiotic contaminants. *Mar. Environ. Res.* 50: 517–521; 2000.
- Freshney R. I. Culture of animal cells: a manual of basic technique and specialized applications. 5th ed. Wiley, Hoboken; 2005.
- Gao A.; Zhou K. Geographical variation of external measurements and three subspecies of *Neophocaena phocaenoides* in Chinese waters. *Acta Theriologica Sinica* 15: 81–92; 1995.
- Guo J. River dolphins down for the count, and perhaps out. *Science* 314: 1860–1860; 2006.
- Hahn W.; Dessain S. et al. Enumeration of the Simian virus 40 early region elements necessary for human cell transformation. *Mol. Cell. Biol.* 22: 2111–2123; 2002.
- Hansen M.; Nielsen S. et al. Re-examination and further development of a precise and rapid dye method for measuring cell growth/cell kill. *J. Immunol. Methods* 119: 203–210; 1989.
- Hayflick L.; Moorhead P. The serial cultivation of human diploid cell strains. *Exp. Cell Res.* 25: 585–621; 1961.
- He F. Price of prosperity: economic development and biological conservation in China. *J. Appl. Ecol.* 46: 511–515; 2009.
- Heinzelmann L.; Chagastelles P. et al. The karyotype of Franciscana dolphin (*Pontoporia blainvillei*). *J. Hered.* 100: 119–122; 2008.
- Holt W.; Pickard A. Role of reproductive technologies and genetic resource banks in animal conservation. *Rev. Reprod.* 4: 143–150; 1999.
- Jaramillo-Legorreta A.; Rojas-Bracho L. et al. Saving the Vaquita: immediate action, not more data. *Conserv. Biol.* 21: 1653–1655; 2007.
- Jefferson T.; Hung S. Effects of biopsy sampling on Indo-Pacific humpback dolphins (*Sousa chinensis*) in a polluted coastal environment. *Aquat. Mamm.* 34: 310–316; 2008.
- Kadoi K.; Mochizuki A. et al. Susceptibility of a line of dolphin kidney cell culture to several herpesviruses. *J. Basic Microbiol.* 32: 227–232; 1992.
- Leon-Quinto T.; Simon M. et al. Developing biological resource banks as a supporting tool for wildlife reproduction and conservation: the Iberian lynx bank as a model for other endangered species. *Anim. Reprod. Sci.* 112: 347–361; 2009.
- Li L.; Guan W. et al. Establishment and characterization of a fibroblast cell line derived from Texel sheep. *Biochem. Cell Biol.* 87: 485–492; 2009.
- Marsili L.; Fossi M. et al. Skin biopsies for cell cultures from Mediterranean free-ranging cetaceans. *Mar. Environ. Res.* 50: 523–526; 2000.
- Menon G.; Grayson S. et al. Lipokeratinocytes of the epidermis of a cetacean (*Phocena phocena*). *Cell Tissue Res.* 244: 385–394; 1986.
- Mosmann T. Rapid colorimetric assay for cellular growth and survival: application to proliferation and cytotoxicity assays. *J. Immunol. Methods* 65: 55–63; 1983.
- Nielsen O.; Kelly R. et al. Some properties of a finite cell line from beluga whale (*Delphinapterus leucas*). *Can. J. Fish. Aquat. Sci.* 46: 1472–1477; 1989.
- Pavelic Z.; Slocum H. et al. Colony growth in soft agar of human melanoma, sarcoma, and lung carcinoma cells disaggregated by mechanical and enzymatic methods. *Cancer Res.* 40: 2160–2164; 1980.
- Pfeiffer C.; Jones F. Epidermal lipid in several cetacean species: ultrastructural observations. *Anat. Embryol.* 188: 209–218; 1993.
- Pine M.; Greer K. et al. Comparison of reactive oxygen scavenging systems between a cetacean (DKN1) and a porcine renal epithelial cell line (LLC-PK1). *Comp. Biochem. Physiol. Part A Mol. Integr. Physiol.* 147: 550–555; 2007.
- Pine M.; Schroeder M. et al. Generation and partial characterization of a transformed cetacean cell line. *Aquat. Toxicol.* 67: 195–202; 2004.
- Reeb D.; Best P. et al. Structure of the integument of southern right whales, *Eubalaena australis*. *Anat. Rec Part A* 290: 596–613; 2007.
- Rundell K.; Parakati R. The role of the SV40 ST antigen in cell growth promotion and transformation. *Semin. Cancer Biol.* 11: 5–13; 2001.
- Russell W.; Newman C. et al. A simple cytochemical technique for demonstration of DNA in cells infected with mycoplasmas and viruses. *Nature* 253: 461–462; 1975.
- Seabright M. The use of proteolytic enzymes for the mapping of structural rearrangements in the chromosomes of man. *Chromosoma* 36: 204–210; 1972.
- Shi L. Freezing zoo-establishment and application of wild animal cell banks. *Biol. Bull.* 6: 1–3; 1989.
- Silva R.; Zahra D. et al. Immortalization of human fibroblasts by liposome-mediated transfer of SV40 early region genes. *Methods Cell Sci.* 17: 75–81; 1995.

- Smith A.; Skilling D. et al. Serology and virology of the bowhead whale (*Balaena mysticetus* L.). *J. Wildl. Dis.* 23: 92–98; 1987.
- Stewart S.; Weinberg R. Senescence: does it all happen at the ends? *Oncogene* 21: 627–630; 2002.
- Stewart S.; Weinberg R. Telomeres: cancer to human aging. *Annu. Rev. Cell Dev. Biol.* 22: 531–557; 2006.
- Stone R. Conservation biology: last stand on the Yangtze. *Science* 329: 378; 2010.
- Strickland J.; Bailey E. et al. Assessment of the mitogenic potential of the alkaloids produced by endophyte (*Acremonium coenophialum*)-infected tall fescue (*Festuca arundinacea*) on bovine vascular smooth muscle in vitro. *J. Anim. Sci.* 74: 1664–1671; 1996.
- Sutherland W. J.; Adams W. M. et al. One hundred questions of importance to the conservation of global biological diversity. *Conserv. Biol.* 23: 557–567; 2009.
- Turvey S.; Pitman R. et al. First human-caused extinction of a cetacean species? *Biol. Lett.* 3: 537; 2007.
- Walen K.; Madin S. Comparative chromosome analyses of the bottlenosed dolphin (*tursiops truncatus*) and the pilot whale (*globicephala scammonii*). *Am. Nat.* 99: 349–354; 1965.
- Wang D. Population status, threats and conservation of the Yangtze finless porpoise. *Chin. Sci. Bull.* 54: 3473–3484; 2009.
- Wang D.; Zhang X. et al. Conservation of the Baiji: no simple solution. *Conserv. Biol.* 20: 623–625; 2006.
- Weller D.; Cockcroft V. et al. Behavioral responses of bottlenose dolphins to remote biopsy sampling and observations of surgical biopsy wound healing. *Aquat. Mamm.* 23: 49–58; 1997.
- Widera D.; Zander C. et al. Adult palatum as a novel source of neural crest-related stem cells. *Stem Cells* 27: 1899–1910; 2009.
- Wiidt D. Genetic resource banks for conserving wildlife species: justification, examples and becoming organized on a global basis. *Anim. Reprod. Sci.* 28: 247–257; 1992.
- Wilson J.; Sargent J. et al. A feasibility study of the MTT assay for chemosensitivity testing in ovarian malignancy. *Br. J. Cancer* 62: 189; 1990.
- Wise J.; Wise S. et al. Hexavalent chromium is cytotoxic and genotoxic to the North Atlantic right whale (*Eubalaena glacialis*) lung and testes fibroblasts. *Mutat. Res.* 650: 30–38; 2008.
- Yu J.; Kindy M. et al. Establishment of epidermal cell lines derived from the skin of the Atlantic bottlenose dolphin (*Tursiops truncatus*). *Anat. Rec Part A* 287: 1246–1255; 2005.
- Zhao X.; Barlow J. et al. Abundance and conservation status of the Yangtze finless porpoise in the Yangtze River, China. *Biol. Conserv.* 141: 3006–3018; 2008.